



UNIVERSITY OF LEEDS

This is a repository copy of *Phosphorylation-induced unfolding regulates p19(INK4d) during the human cell cycle*.

White Rose Research Online URL for this paper:  
<http://eprints.whiterose.ac.uk/132698/>

Version: Accepted Version

---

**Article:**

Kumar, A, Gopalswamy, M, Wolf, A et al. (3 more authors) (2018) Phosphorylation-induced unfolding regulates p19(INK4d) during the human cell cycle. *Proceedings of the National Academy of Sciences of the United States of America*, 115 (13). pp. 3344-3349. ISSN 0027-8424

<https://doi.org/10.1073/pnas.1719774115>

---

© 2018. This is an author produced version of a paper published in *Proceedings of the National Academy of Sciences of the United States of America*. In order to comply with the publisher requirements the University does not require the author to sign a nonexclusive licence for this paper. Uploaded in accordance with the publisher's self-archiving policy.

**Reuse**

Items deposited in White Rose Research Online are protected by copyright, with all rights reserved unless indicated otherwise. They may be downloaded and/or printed for private study, or other acts as permitted by national copyright laws. The publisher or other rights holders may allow further reproduction and re-use of the full text version. This is indicated by the licence information on the White Rose Research Online record for the item.

**Takedown**

If you consider content in White Rose Research Online to be in breach of UK law, please notify us by emailing [eprints@whiterose.ac.uk](mailto:eprints@whiterose.ac.uk) including the URL of the record and the reason for the withdrawal request.



[eprints@whiterose.ac.uk](mailto:eprints@whiterose.ac.uk)  
<https://eprints.whiterose.ac.uk/>

# Phosphorylation-induced unfolding regulates p19<sup>INK4d</sup> during the human cell cycle

Amit Kumar<sup>1,2,4</sup>, Mohanraj Gopalswamy<sup>1</sup>, Annika Wolf<sup>3</sup>, David J. Brockwell<sup>2</sup>, Mechthild  
Hatzfeld<sup>3</sup>, Jochen Balbach<sup>1,4,\*</sup>

<sup>1</sup> Institute of Physics, Biophysics, Martin-Luther-University Halle-Wittenberg, 06120 Halle  
(Saale), Germany

<sup>2</sup> Astbury Centre for Structural Molecular Biology, School of Molecular and Cellular  
Biology, Faculty of Biological Sciences, University of Leeds, Leeds LS2 9JT, UK

<sup>3</sup> Institute for Molecular Medicine, Patho-biochemistry, Martin-Luther-University Halle-  
Wittenberg, 06097 Halle (Saale), Germany

<sup>4</sup> Centre for Structure und Dynamics of Proteins (MZP), Martin-Luther-University Halle-  
Wittenberg, Germany

\*Correspondence should be addressed to

Jochen Balbach	Phone: +49 345 55 28550
Institute of Physics, Biophysics	FAX: +49 345 55 27161
Martin-Luther-University Halle-Wittenberg	Email: jochen.balbach@physik.uni-
halle.de	
D-06099 Halle(Saale), Germany	

## **Abstract**

Cell cycle progression is tightly regulated by cyclin–dependent kinases (CDKs). The ankyrin-repeat protein p19<sup>INK4d</sup> functions as a key regulator of G1/S transition, however, its molecular mode of action is unknown. Here, we combine cell and structural biology methods to unravel the mechanism by which p19<sup>INK4d</sup> controls cell cycle progression. We delineate how the stepwise phosphorylation of p19<sup>INK4d</sup> Ser66 and Ser76 by cell cycle independent (p38) and dependent protein kinases (CDK1), respectively, leads to local unfolding of the three N-terminal ankyrin repeats of p19<sup>INK4d</sup>. This dissociates the CDK6-p19<sup>INK4d</sup> inhibitory complex and, thereby, activates CDK6. CDK6 triggers entry into S-phase, whereas p19<sup>INK4d</sup> is ubiquitinated and degraded. Our findings reveal how signaling-dependent p19<sup>INK4d</sup> unfolding contributes to the irreversibility of G1/S transition.

**Key words:** cell cycle/p19<sup>INK4d</sup>/protein unfolding/protein phosphorylation/NMR spectroscopy

## Significance

Cell cycle progression is tightly controlled in healthy organisms and often perturbed in human diseases including, most prominently, in many forms of cancers. Cyclin-dependent protein kinases (CDKs) and their inhibitors, such as p19<sup>INK4d</sup>, regulate the different stages of the cell cycle. Here, we demonstrate how sequential phosphorylation of p19<sup>INK4d</sup> at two sites first destabilizes and then unfolds the N-terminal half of the protein, which dissociates its CDK-inhibitory complex and primes p19<sup>INK4d</sup> for cellular degradation. Our results define a structural mechanism by which phosphorylation-induced protein unfolding controls a key step in cell cycle progression.

**\body**

## **Introduction**

Cell cycle progression from G1 to S-phase is tightly coupled to the transcriptional control of genes involved in growth and DNA replication [1]. In mammalian cells, G1/S transition is primarily mediated by the E2F family of transcription factors [2]. E2F proteins E2F1 to E2F8 form heterodimeric E2 promoter-binding-protein-dimerization partner complexes (E2F-DP) with members of the distantly related DP family of proteins [3]. Most E2F proteins harbor dedicated protein binding domains that interact with E2F targets upon phosphorylation [4] to form inactive, ternary E2F-DP complexes [5] that stall cells in G1. Such cascades also prevent cells from replicating damaged DNA [6]. To successfully enter S phase, CDK-cyclin complexes [7] hyper-phosphorylate [5] and disrupting the E2F-DP assemblies [8] and, in turn, activate E2F-dependent gene expression necessary for G1/S transition (Figure 1). Therefore, CDKs such as CDK4/6 play major roles in cell cycle progression. CDK4/6 are controlled via their regulatory subunits including D-type cyclins and specific cyclin dependent kinase inhibitors (CKIs), of which two families are known. Specifically, CKIs belonging to the INK4 family of proteins (p16<sup>INK4a</sup>, p15<sup>INK4b</sup>, p18<sup>INK4c</sup>, and p19<sup>INK4d</sup>) (Figure 1) inhibit CDK4 and CDK6, whereas CKIs of the Cip/Kip family (p21<sup>Cip1, WAF-1</sup>, p27<sup>Kip1</sup>, p57<sup>Kip2</sup>) act on CDK2 and other CDKs [7, 9, 10]. p19<sup>INK4d</sup> has distinct features compared to the other four members of the INK4 family; mRNA and protein levels accumulate during S phase and sharply decline at the onset of G2. High amounts of p19<sup>INK4d</sup> inhibit CDK4/6-cyclin D activity and determine the length of G1, also ensuring the directionality of cell cycle progression [7]. In exponentially growing U2OS cells, p19<sup>INK4d</sup> is found to be phosphorylated at two sites, tentatively assigned to Ser66 and Ser76 [11]. Additional regulation by ubiquitination appears to be restricted to p19<sup>INK4d</sup> and thought to involve Lys62 and depend on CDK4 binding. Given that cellular

concentrations of p19<sup>INK4d</sup> oscillate during the cell cycle, it has been proposed that regulated modification events at these sites determine the fate of intracellular p19<sup>INK4d</sup> [11].

In-cell NMR allows the study of proteins and their post-translational modifications in cellular environments [12-14]. Alternatively, purified isotope-labeled proteins of interest may be added directly to unlabeled, native cell lysates to study how endogenous cellular proteins such as kinases, phosphatases or proteases act on them [15, 16]. Here, we adopted the latter approach to gain mechanistic insights into the phosphorylation behavior of full-length human p19<sup>INK4d</sup> and to interrogate structural and functional consequences of such modifications. We show that p19<sup>INK4d</sup> Ser66 and Ser76 are phosphorylated by cellular p38 and CDK1 in a strictly stepwise and cell cycle-dependent manner. In response, p19<sup>INK4d</sup> locally unfolds and dissociates from CDK6, which triggers Lys62 ubiquitination and, ultimately, leads to cellular p19<sup>INK4d</sup> degradation. Hence, we demonstrate how the combined use of cell biology and NMR spectroscopy enables novel insights into the molecular mechanisms that regulate p19<sup>INK4d</sup> activity during cell cycle progression..

## Results

**p19<sup>INK4d</sup> phosphorylation at Ser66.** p19<sup>INK4d</sup> is an ankyrin-repeat (AR) protein that harbors five evenly spaced helix-turn-helix motifs AR1 aa9–29, AR2 aa54–62, AR3 aa77–95, AR4 aa110–128, and AR5 aa142–159 (Fig 1A). AR1 and AR2 mediate inhibitory CDK4/6 binding [17]. Phosphorylation of Ser66 and Ser76 within the linker region connecting AR2 and AR3 is thought to regulate p19<sup>INK4d</sup> activity, but kinases that modify these sites have not been identified. We expressed and purified full-length human p19<sup>INK4d</sup> (residues 1–166) from *E. coli* and added the recombinant protein to lysates that we prepared from various cultured cell lines, e.g. HeLa, U2OS, HEK–293 grown asynchronously, and from *Drosophila melanogaster* embryos. <sup>32</sup>P-incorporation and autoradiography exposure confirmed phosphorylation by endogenous enzymes (Figure S1A). To identify respective p19<sup>INK4d</sup> phosphorylation sites, we similarly prepared <sup>15</sup>N-isotope labelled protein that we added to corresponding lysates for 3 h, before we directly recorded 2D <sup>1</sup>H–<sup>15</sup>N HSQC (heteronuclear single–quantum coherence) and 1D <sup>31</sup>P NMR spectra on the resulting lysate mixtures. The NMR resonance assignment of p19<sup>INK4d</sup> has previously been reported [18] (Figure S2F). Because NMR chemical shifts are sensitive indicators of residue-specific chemical environments, phosphorylation-induced chemical shift changes conveniently identify the respective modification sites. One added benefit of detecting protein phosphorylation by NMR is that conformational rearrangements occurring in response to such modifications result in additional chemical shift changes that are readily interpretable also in structural terms. Incubation of p19<sup>INK4d</sup> in each of the four lysates resulted in the phosphorylation of p19<sup>INK4d</sup>, manifested by pronounced chemical shift changes of Ser66 resonance signals (Figure 2A, shown for HeLa cells lysate, and Figures S1B–D). Although residues close to Ser66 also displayed slight alterations in their cross peak positions (red in Figure 2A), other p19<sup>INK4d</sup> serines, including Ser76, were unaffected. These results indicated that all five ankyrin repeats remained structurally intact upon Ser66 phosphorylation. In the 1D <sup>31</sup>P NMR spectrum, phospho-Ser66 gave rise to a characteristic

new resonance at  $-2$  ppm, which was clearly offset from the bulk phosphate-buffer signal at  $2$  ppm (inset in Figure 2A). We confirmed the presence of a single protein-phosphate moiety by MALDI-TOF mass spectrometry (Figures S2A and B). To verify the identity of Ser66 as the primary phosphorylation site, we repeated these experiments with alanine-substituted, mutant p19<sup>INK4d</sup> (e.g. S66A). We neither detected  $^{32}\text{P}$  incorporation, nor the appearance of the  $^{31}\text{P}$ -NMR resonance signal at  $-2$  ppm. These data confirmed that endogenous kinases in lysates prepared from asynchronously growing mammalian cells, or from *Drosophila* embryos, phosphorylated p19<sup>INK4d</sup> at Ser66.

**Stepwise phosphorylation of Ser66 and Ser76 induces local unfolding.** Having preformed the previous set of experiments in lysates of asynchronously growing cells, we were unable to delineate cell cycle-specific contributions to the observed phosphorylation reaction. To our surprise, we also did not detect endogenous p19<sup>INK4d</sup> in our lysates (Figure S2C, lane 1). Because G1/S transition is tightly controlled by CDK4/6 and INK4, we speculated that the kinase targeting p19<sup>INK4d</sup> might only be active in a fraction of our collected cells, specifically those in S-phase. To test this hypothesis, we subjected HeLa cells to a double thymidine block to arrest them in S-phase [19]. We detected abundant amounts of endogenous p19<sup>INK4d</sup> in these lysates (Figure S2C, lane 2). Upon thymidine removal and G2 release, p19<sup>INK4d</sup> levels dropped below the detection limit within 6 h (Figure S2C, lane 3 and 4). These findings reaffirmed earlier studies with proliferating cells [20] that cellular p19<sup>INK4d</sup> concentrations were highest in S-phase and virtually absent in G1, thus consolidating the notion of a genuine oscillatory behavior.

Next, we sought to investigate p19<sup>INK4d</sup> modifications in lysates of S-phase arrested cells.  $^{32}\text{P}$  incorporation and autoradiography exposure confirmed p19<sup>INK4d</sup> phosphorylation (Figure S2D). 1D  $^{31}\text{P}$  NMR experiments revealed the previously observed phospho-resonance at  $-2$  ppm, plus a new signal at  $+4$  ppm suggesting the presence of a second modified residue under

these conditions (inset in Figure 2B). MALDI-TOF mass spectrometry indeed confirmed phosphorylation of p19<sup>INK4d</sup> at two sites (Figures S2A and E). To also interrogate possible structural changes of doubly phosphorylated p19<sup>INK4d</sup>, we recorded 2D <sup>1</sup>H–<sup>15</sup>N HSQC spectra on exogenously added, isotope-labeled protein in lysates of S-phase arrested HeLa cells (Figure 2B). Surprisingly, we found all p19<sup>INK4d</sup> residues of AR1, AR2 and AR3 at new peak positions, narrowly dispersed around 8 ppm. along the proton dimension (Figures 2B and S2F). Such NMR features are highly characteristic of unfolded protein states. By contrast, residues within AR4 and AR5 exhibited no chemical shift changes indicating that these ankyrin repeats remained folded upon dual p19<sup>INK4d</sup> phosphorylation. Having established that Ser66 likely constituted one of the modified p19<sup>INK4d</sup> residues, we set out to identify the second phosphorylation site. To this end, we mutated Ser76 to alanine (S76A) and repeated the S-phase lysate NMR experiment. 2D <sup>1</sup>H–<sup>15</sup>N HSQC spectra showed that AR1–3 residues, along with those of AR4 and AR5, maintained their original cross peak positions, hinting towards the structural preservation of all ankyrin-repeats (Figures 3F and S2G). Moreover, we clearly detected Ser66 phosphorylation in S76A p19<sup>INK4d</sup> suggesting that primary phosphorylation of this site was not affected in the mutant background. Together, these results led us to conclude that Ser76 constituted the second p19<sup>INK4d</sup> modification site in S-phase arrested cell extracts, that phosphorylation of Ser66 pursued independent of Ser76 modification, and that double phosphorylation of Ser66 and Ser76 resulted in local unfolding of ankyrin repeats 1–3.

To confirm that the observed conformational changes were indeed due to phosphorylation, and to test whether local AR1-3 unfolding was reversible, we added a non-specific alkaline phosphatase to Ser66-, Ser76-modified p19<sup>INK4d</sup>. Dephosphorylation resulted in the disappearance of phospho–protein resonances in 1D <sup>31</sup>P NMR spectra (inset in Figure 2C) and recovered all p19<sup>INK4d</sup> resonances at their original cross peak positions in 2D <sup>1</sup>H–<sup>15</sup>N HSQC spectra (Figure 2C and 3C). These experiments confirmed that i) double phosphorylation

caused unfolding and ii) that unfolding was fully reversible. They further excluded contributions by other post-translational protein modifications, which may have remained undetected in lysate NMR experiments.

**p38 and CDK1 phosphorylate Ser66 and Ser76, respectively.** We observed Ser66 phosphorylation in lysates of asynchronously growing cells, as well as in lysates of cells arrested in S-phase, which suggested that this modification is mediated by a kinase that is not stringently cell cycle-regulated. By contrast, we only detected Ser76 phosphorylation in S-phase lysates, arguing for an enzyme with cell cycle-specific activity. To identify the respective kinases that modified Ser66 and Ser76 of p19<sup>INK4d</sup>, we treated S-phase lysates with different kinase inhibitors. Compounds targeting CDK1, CDK4 or protein kinase A (PKA) did not affect Ser66 phosphorylation (Figures S3A – C). By contrast, selective inhibition of the constitutively expressed kinase p38 [21-23] abolished its modification (Figures 3E and S3D). We further confirmed p38 selectivity and specificity in reconstituted kinase reactions with isolated wild-type and S66A-mutant p19<sup>INK4d</sup> (Figure S3E). Furthermore, in an autoradiography experiment, p19<sup>INK4d</sup> S66A remained silent (Figure S3E). p38 is a stress-activated MAP kinase protein family and we found Ser66 to get phosphorylated under various conditions not related to the cell-cycle. Therefore, p38 may not be the only kinase that phosphorylates Ser66.

Following a similar approach, we found that different CDK1 inhibitors abolished Ser76 phosphorylation, whereas modification of Ser66 was unperturbed (Figures 3D, S4A and S4B). In earlier studies, CDK2 was found to phosphorylate Ser76 in DNA damage response [24]. The here used CDK1 inhibitor IV inhibits CDK2 to some extent at elevated concentrations [25] but specific CDK1 inhibitor III does not [26]. Sole inhibition of CDK2 by inhibitor I (Fig S4C) and, as expected, treating S-phase cell lysates with CDK4 or PKA inhibitors showed no effects (Figures S4D and S4E). Together, these results suggested that predominantly CDK1

mediated Ser76 phosphorylation. Accordingly, we found that CDK1-cyclin B reconstituted kinase reactions modified wild-type but not S76A-mutant p19<sup>INK4d</sup> (Figure S5A). CDK1, in complex with cyclins A, B, D or E, functions as a key cell cycle regulator [27-29] and p19<sup>INK4d</sup> exhibits several features of a canonical CDK1 substrate [30]. It harbors multiple serine or threonine residues followed by a proline, e.g. minimal Ser/Thr-Pro motifs, including Ser66, Ser76 and Thr141, and it contains a classical Arg-X-Leu CDK docking site, which all remain accessible even when p19<sup>INK4d</sup> is bound to CDK4/6 (Figure 1, left). To further substantiate the role of CDK1 in Ser76 phosphorylation, we arrested HeLa cells in M-phase, in which CDK1/cyclin B activity is the highest, and prepared lysates to which we added <sup>15</sup>N isotope-labeled p19<sup>INK4d</sup>. 2D NMR experiments revealed local unfolding of AR1-3, manifested by spectral characteristic that were indistinguishable from results in S-phase arrested cell extracts (Figures S5B-S5D). Indeed, NMR spectra of isotope-labeled p19<sup>INK4d</sup> in reconstituted mixtures of isolated p38 $\alpha$  and CDK1/cyclin B showed identical features (Figures S6A - F). In summary, our combined results strongly suggested that p38 and CDK1 constitute the cellular kinases that phosphorylate Ser66 and Ser76 of p19<sup>INK4d</sup>, respectively.

**p19<sup>INK4</sup> phosphorylation is a two step process.** Having identified p38 and CDK1 as likely kinase candidates for cellular p19<sup>INK4d</sup> phosphorylation, we set out gain mechanistic insights into the Ser66 and Ser76 modification process. Specifically, we asked whether Ser76 phosphorylation required Ser66 modification as a preceding event. We had found that phosphorylation of Ser76 did not occur in the S66A-mutant background (Figure 3G) or upon p38 inhibition in S-phase cell lysates (Figures 3H, S7A, and S7B), thus raising the possibility that Ser66, Ser76 phosphorylation may constitute a hierarchical, sequential process. Protein phosphorylation sites are generally located in accessible loop and linker regions of folded substrates [30]. In p19<sup>INK4d</sup>, Ser66 is surface-exposed whereas Ser76 is part of the helical AR3 motif and rather occluded (Figure 1, left). As mentioned above, Ser66 phosphorylation led to

several NMR chemical shift changes of residues in its vicinity (Figure 2A). We hypothesized that these reported on local destabilization of p19<sup>INK4d</sup> residues surrounding the modification site, probably via repulsive electrostatic interactions of the Ser66 phosphate moiety and the negative charge of the net dipole moments at the C-terminal ends of helices 4 and 6 in AR2 and AR3, respectively (Figure 2A and arrows on the corresponding p19<sup>INK4d</sup> structure). In agreement with this model, residues in these helices displayed the largest chemical shift changes upon Ser66 phosphorylation (Figure 2A). To assess the degree of helix destabilization in response to Ser66 modification, we performed proton-deuteron (H-D) backbone amide exchange experiments by NMR. AR3 and AR4 residues in wild-type p19<sup>INK4d</sup> exhibited protection factors above 10<sup>5</sup> (Figure S7C and [31]), which reduced significantly upon phosphorylation (red in Figure S7D and Figures S7E and F). Surprisingly, even though p19<sup>INK4d</sup> residues within AR1, 4 and 5 did not show chemical shift changes when Ser66 was phosphorylated, we measured greater solvent-amide proton exchange at these ‘remote’ structural elements, synonymous with lower thermodynamic stabilities in the presence of modified Ser66. Based on these findings, we hypothesized that extended structural destabilization may provide the necessary access for Ser76 phosphorylation by CDK1 (Figure 1). Local unfolding of AR1–3 may then occur due to additional breaking of hydrogen bonds, such as the one between Ser76 O<sup>γ</sup> and V69 O<sup>γ</sup>, for example.

**Phosphorylation dissociates the CDK6–p19<sup>INK4d</sup> complex.** How does p19<sup>INK4d</sup> phosphorylation correlate with its function as cell cycle regulator? The crystal structure of the inhibitory CDK6–p19<sup>INK4d</sup> complex reveals its molecular architecture [17] but it had remained unclear how the assembly dissociates and whether p19<sup>INK4d</sup> modifications affected this process. Therefore, we examined p19<sup>INK4d</sup> phosphorylation in context of the assembled CDK6–p19<sup>INK4d</sup> complex. In vitro pull down assays showed that unmodified p19<sup>INK4d</sup> specifically bound to GST–CDK6 [31], whereas doubly phosphorylated p19<sup>INK4d</sup> did not

(Figure 4A), likely because a folded AR1–2 interface is required for CDK6 binding (Figure 1, left). In a second experiment, we followed  $^{15}\text{N}$ -p19<sup>INK4d</sup> binding to unlabeled CDK6 by NMR spectroscopy. As we expected from the crystal structure of the complex, p19<sup>INK4d</sup> AR1 and AR2 residues exhibited pronounced chemical shift changes upon addition of CDK6 (Figures 4B and C). No chemical shift changes were observed when we added CDK6 to doubly phosphorylated p19<sup>INK4d</sup>, which confirmed the absence of binding and recapitulated our pull-down results. When we treated assembled CDK6– $^{15}\text{N}$ -p19<sup>INK4d</sup> with S-phase arrested cell lysates, 2D NMR spectra revealed local unfolding of AR1-3 similar to the isolated protein upon Ser66 and Ser76 phosphorylation (Figure 4D, middle). Indeed, 1D  $^{31}\text{P}$  NMR spectra and radioisotope incorporation experiments confirmed the presence of both modifications (Figure 4D, bottom). We concluded that p19<sup>INK4d</sup> double phosphorylation and subsequent local unfolding dissociated the p19<sup>INK4d</sup>-CDK6 complex.

**Ubiquitination requires p19<sup>INK4d</sup> unfolding.** Many proteins turn into E3 ubiquitin ligases substrates upon phosphorylation causing them to be degraded by the ATP-dependent ubiquitin/proteasome system [32, 33]. Here, we showed that p19<sup>INK4d</sup> phosphorylation at Ser66 and Ser76 caused local unfolding of AR1-3, which, in turn, released the protein from CDK6. What was the cellular fate of free doubly modified p19<sup>INK4d</sup>? We reasoned that the locally unfolded protein may become ubiquitinated and eventually degraded, which would explain the rapid disappearance of endogenous p19<sup>INK4d</sup> in lysates of cells released from S-phase arrest (Figure S2C). Indeed, this drop of endogenous p19<sup>INK4d</sup> level upon thymidine removal and G2 release could be prevented by CDK1 inhibition during S phase (Figure 5), confirming the coupling between Ser76 phosphorylated p19<sup>INK4d</sup> and its cell cycle- dependent degradation.

In line with this model, we expected AR1-3 unfolding to also expose Lys62, a canonical ubiquitination site of p19<sup>INK4d</sup>. To test this hypothesis, we performed in vitro ubiquitination

assays with S-phase arrested cell lysates and pre-phosphorylated p19<sup>INK4d</sup>. We did not detect ubiquitination of unmodified or Ser66-phosphorylated protein. Only Ser66 and Ser76-phosphorylated p19<sup>INK4d</sup> was evidently modified (Figure S8). As expected, neither S66A nor S76A-mutant p19<sup>INK4d</sup> was ubiquitinated.

In summary, these findings (Figure 6) suggested that cellular ubiquitination of p19<sup>INK4d</sup> likely depended on its phosphorylation and concomitant structural state. In support of our hypothesis, we concluded that cell cycle-dependent, stepwise phosphorylation of Ser66 and Ser76 induced local unfolding of AR1–3, which, in turn, dissociated p19<sup>INK4d</sup> from CDK6 and exposed Lys62 for subsequent ubiquitination, which likely served as the signal for intracellular degradation.

## Discussion

To initiate G1/S transition, CDK4/6 phosphorylates trigger factors such as the retinoblastoma Rb protein, which in turn release E2F transcription factors required for cell cycle progression (Figure 1). Unmodified p19<sup>INK4d</sup> binds CDK4/6 and inhibits its function [34]. Multisite phosphorylation of INK4 proteins such as p19<sup>INK4d</sup> and p18<sup>INK4c</sup> in asynchronously growing cells has been observed previously [11, 34] and characterized in vitro by Ser to Glu substitutions mimicking phosphorylation [35], but the functional consequences of these modifications remained enigmatic. Here, we established that phosphorylation of p19<sup>INK4d</sup> Ser66 by p38 kinase broadly destabilizes N-terminal ankyrin repeats, which appears to constitute a necessary priming event for the stepwise modification of Ser76 by CDK1. Double phosphorylation induces local unfolding of p19<sup>INK4d</sup> ankyrin repeats 1-3, which dissociates the inhibitory CDK4/6-p19<sup>INK4d</sup> complex. In turn, modified, free and unfolded p19<sup>INK4d</sup> undergoes ubiquitination, which predestines the protein for cellular degradation. A schematic summary of this process is depicted in Figure 6. One key feature of this model is the switch-like function that the cell cycle-dependent protein kinase CDK1 imposes on the network. Clearly, CDK1-mediated phosphorylation of p19<sup>INK4d</sup> Ser76 appears to determine the functional outcome of the entire regulatory hub. In the absence of CDK1 activity, and Ser76 phosphorylation, p19<sup>INK4d</sup> blocks cell cycle progression by binding to CDK4/6 and, thereby, inhibits their functions. In this regard, the cell cycle-independent, primary phosphorylation of p19<sup>INK4d</sup> Ser66 maintains the system in a poised state that is primed for activation by CDK1. Once CDK1 activity is triggered, p19<sup>INK4d</sup> Ser76 phosphorylation frees CDK4/6 for transcriptional activation cumulating in cell cycle progression. At the same time, doubly phosphorylated p19<sup>INK4d</sup> undergoes ubiquitination and eventual degradation, which ensures the irreversibility of the process and, by proxy, the directionality of the cell cycle.

Maybe one of the most striking features of this regulatory network is its structural component. Whereas phosphorylation of the primary p19<sup>INK4d</sup> substrate site (Ser66) destabilizes structured ankyrin repeats more globally and, thereby, ‘enables’ secondary site (Ser76) modification, the actual phosphorylation event ‘executes’ the functional reprogramming step, which is largely driven by a local loss-of-structure mechanism. Unfolding not only disrupts the CDK4/6-p19<sup>INK4d</sup> complex and, thereby, activates these kinases, it also exposes the previously buried p19<sup>INK4d</sup> Lys62 residue for ubiquitination, which initiates p19<sup>INK4d</sup> degradation and clearance. At this level of post translational modifications, differences between the four INK4 members are evident, which are not related to the cell cycle dependent mRNA levels [20]. P18<sup>INK4c</sup> declines much more slowly as cells advance through G1/S phase compared to p19<sup>INK4d</sup>. The major ubiquitin acceptors Lys46 and Lys112 are buried in p18<sup>INK4c</sup> ankyrin repeats AR2 and AR4, and this INK4 member lacks any S/T-P motif. Therefore, we speculate that the much shorter cellular half-life of p19<sup>INK4d</sup> results from the here disclosed mechanism of Lys62 exposure.

Differences in the thermodynamic stabilities of individual ankyrin repeats in other AR-containing proteins were found to determine the folding pathways [31] of the NF- $\kappa$ B inhibitor I $\kappa$ B $\alpha$  [36], the Notch receptor [37] and tANK [38]. However, these examples undergo structural rearrangements in absence of post-translational modifications. Phosphorylation-induced unfolding of p19<sup>INK4d</sup> is uniquely mediated by two sequential modification steps, which jointly dissolve the N-terminal half of this classically folded protein domain. To our knowledge, there exists only one other example of phosphorylation-mediated destruction of a fully structured protein entity, which is the KH1 domain of the K-homology splicing regulator protein KSRP [39]. In that case, insertion of a negative charge at a single serine residue (Ser193) disrupts the globular KH1 fold and, in turn, exposes a linear sequence motif that confers nuclear trans-localization of KSRP.

The S/T-P motif is conserved in the consensus sequence of ankyrin repeats, which structurally well aligns e.g. the INK4 members (p19<sup>INK4d</sup>, p18<sup>INK4c</sup>, p16<sup>INK4a</sup>, p15<sup>INK4b</sup>) with GABP $\beta$ , myotrophin, and 53BP2 [18, 40]. Ser66 is not conserved in any of the other homologs and therefore unique as priming site for p19<sup>INK4d</sup> phosphorylation. The transcription factor GABP  $\beta$  subunit contains 4 ankyrin repeats and it has been speculated that MAPK/ERK mediated phosphorylation involves the S/T-P motifs in AR2 (Ser39-Pro40) and AR3 (Thr73-Pro74) [41], the latter corresponds to Ser76-Pro77 in p19<sup>INK4d</sup>. Along the same lines, among the four ankyrin repeats in myotrophin only AR3 harbors such a motif at Thr70-Pro71, and its phosphorylation has been discussed during initiation of cardiac hypertrophy [42].

Within these structural homologs, only p19<sup>INK4d</sup> contains one further S/T-P motif at position Thr141-Pro142. This threonine was found to be phosphorylated by PKA as DNA damage response following e.g. UV irradiation or cisplatin treatment of cells [24]. A putative priming site is Ser130 between AR5 and AR6 at a structural position homologous to Ser66. Destabilization of scaffold repeats AR5 and AR6 [31, 35] might cause the same unfolding of p19<sup>INK4d</sup> and genotoxic stress induced CDK4/6 release, a hypothesis, which has to be experimentally addressed in the future. These examples document that phosphorylation induced unfolding of ankyrin repeats, typically involved in protein-protein interactions, and as delineated in molecular detail here for p19<sup>INK4d</sup>, might represent an evolutionary conserved principle in cellular signaling.

## Materials and Methods

**Protein expression and purification.** p19<sup>INK4d</sup> wild type (wt) and mutants were expressed in BL21(DE3) pLysS cells and purified as described [31] and further details are provided in SI Materials and Methods.

**Cell lines and synchronization.** Cervical carcinoma (HeLa), human embryonic kidney 293 (HEK-293) and human osteosarcoma (U2OS) cells were employed and synchronization was achieved by double incubation with thymidine (S-phase) or Nocodazole (M-phase). All details are described in SI Materials and Methods.

**Protein assays.** The kinase assay was performed by incubating cell lysate (0.5–1 mg/ml total protein concentration) of exponentially growing or synchronized cells in the presence of <sup>32</sup>P ATP (5 μCi <sup>32</sup>P-γ-ATP) and cAMP (5 μM) with 30 μg of p19<sup>INK4d</sup> for 3 h at 37 °C. Aliquots of the mixtures were analyzed by SDS-PAGE and labeled polypeptides were detected by autoradiography. Further details together with the in vitro kinase assay with isolated p38 or CDK1/cyclin B1, the CDK6-p19<sup>INK4d</sup> pull-down assay and the p19<sup>INK4d</sup> ubiquitination assay are given in SI Materials and Methods.

**NMR spectroscopy experiments.** The cells were lysed as mentioned above in the presence of kinase assay buffer, protease inhibitors and phosphatase inhibitors. The lysate was collected by centrifugation. For the NMR spectroscopy experiment, lysate (15–20 mg/ml) was mixed with 30 μM of <sup>15</sup>N labeled p19<sup>INK4d</sup> or its mutants, 100 μM ATP, and 5 μM cAMP. This reaction mixture was incubated for 3 h at 37 °C. Subsequently, the reaction samples were dialyzed using a 3.5 kDa cut-off membrane in phosphate buffer (20 mM Na<sub>2</sub>HPO<sub>4</sub>, 25 mM NaCl, 25 mM KCl and pH 7.4) for 17 h in order to remove the unincorporated ATP, small molecules and to minimize buffer effects to facilitate a proper chemical shift analysis of NMR cross-peaks. These samples were also analyzed by MALDI-TOF mass spectrometry. Details

about the acquisition of NMR experiments and the  $^1\text{H}/^2\text{H}$  exchange detected by NMR are provided in SI Materials and Methods.

### **Acknowledgments**

We thank Gunter Reuter for *D. melanogaster* embryos, Ernest D. Laue and Wei Zhang for GST–CDK6, Stefan Gröger for NMR spectroscopy support as well as Gary Sawers and René Keil for very helpful discussions. Autoradiography was performed in the Leibniz institute of plant biochemistry Halle. This work has been supported by grants from the DFG (GRK 1026, SFB TRR102), the BMBF (ProNet–T3), and EFRE by the EU.

### **Author contributions**

A.K. and J.B. designed and analyze the experiments. A.K. and M.G. performed the NMR spectroscopy experiments. A.K., A.W. and M.H. designed and performed the cell biology experiments. A.K., D.J.B., M.H. and J.B. wrote the paper.

### **Conflict of interest**

Author declare no conflict of interest

## Figure and Legends

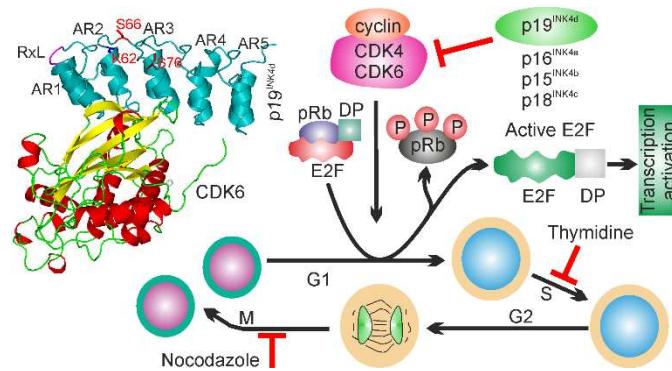


**Figure 1:** Schematic showing the function of p19<sup>INK4d</sup>. Left: structure of the CDK6-p19<sup>INK4d</sup> complex (PDB: 1BLX). Ankyrin repeats of p19<sup>INK4d</sup> are presented as AR1 – AR5, regulatory sites, Ser66, Ser76 and Lys62 are shown red and RxL motif in magenta. Right: the signalling pathways regulated by the INK family members. Red blocks ( $\perp$ ) highlight the cell cycle arrest points used in this study.

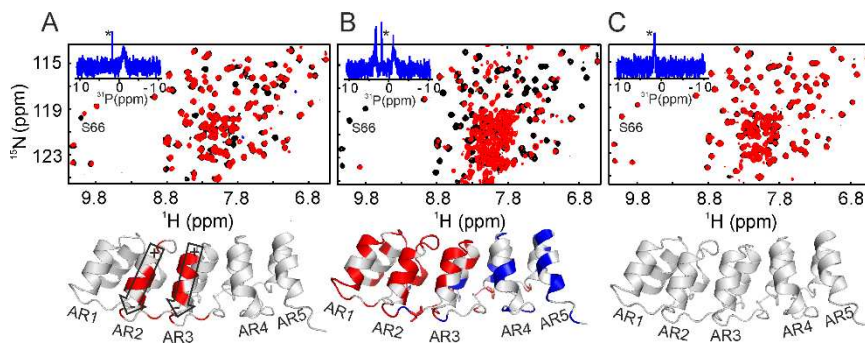


**Figure 2:** NMR detected cell-cycle dependent phosphorylation and local unfolding of p19<sup>INK4d</sup>. Top: overlays of 2D <sup>1</sup>H-<sup>15</sup>N HSQCs of p19<sup>INK4d</sup> before (black) and after (red) incubation with (A) asynchronous cell lysate, (B) S phase HeLa cell lysate or (C) after incubation of the doubly phosphorylated protein by alkaline phosphatase. Bottom: spectral changes upon incubation mapped on the p19<sup>INK4d</sup> structure. The macroscopic helix dipole moments of helix 4 and 6 are depicted by black arrows in (A). Mapping of cross peak on p19<sup>INK4d</sup> structure in (A) and (B): red – missing cross peak, blue – no change and grey slight chemical shift or cannot say. Insets show the 1D <sup>31</sup>P spectra identifying (A) one (–1 ppm), (B) two (–1 ppm and 4 ppm), and (C) no protein-bound phosphate. The sharp signal at 2 ppm originates from the phosphate buffer (asterisk).

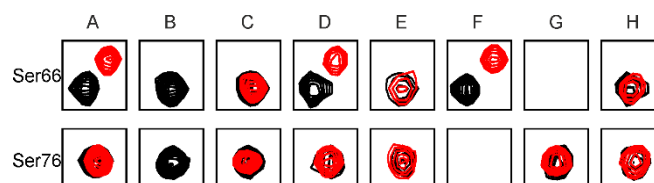


**Figure 3:** Phosphorylation status of Ser66 and Ser76 monitored by NMR spectroscopy. Sections of the overlaid 2D  $^1\text{H}$ - $^{15}\text{N}$  HSQC spectra of p19<sup>INK4d</sup> before (black) and after (red) incubation with cell lysate are depicted. (A) p19<sup>INK4d</sup> incubated in asynchronous HeLa cell lysate (see Figure 2A). (B) p19<sup>INK4d</sup> incubated in S phase HeLa cell lysate (see Figure 2B). (C) Initially doubly phosphorylated p19<sup>INK4d</sup> after incubation with alkaline phosphatase (see Figure 2C). (D) Inhibition of Ser76 phosphorylation by the CDK1 inhibitor IV (p19<sup>INK4d</sup> incubated in S phase HeLa cell lysate). (E) Inhibition of Ser66 phosphorylation by p38 inhibitor SB203580 (p19<sup>INK4d</sup> incubated in asynchronous HeLa cell lysate). (F) p19<sup>INK4d</sup> S76A variant incubated in S phase HeLa cell lysate. (G) p19<sup>INK4d</sup> S66A variant incubated in S phase HeLa cell lysate. (H) p19<sup>INK4d</sup> incubated with S phase HeLa cell lysate in the presence of the p38 inhibitor SB203580. The missing cross-peaks in (F) and (G) are due to the substitution of Ser with Ala at position 76 and 66, respectively. The entire 2D spectrum for each of the eight experiments is depicted in supplementary information.

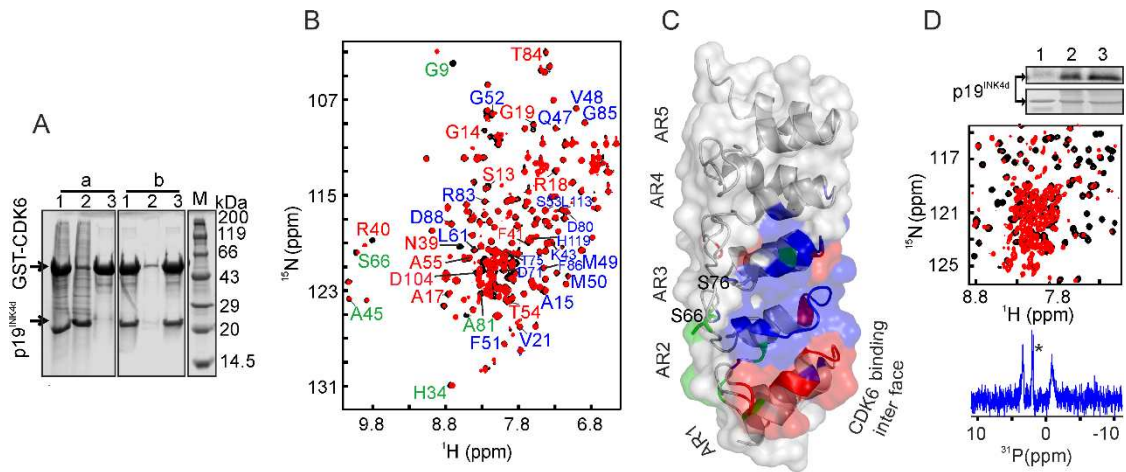


**Figure 4:** Functional implications of p19<sup>INK4d</sup> phosphorylation. (A) Pull-down assay of p19<sup>INK4d</sup> using GST-CDK6. The loading in a and b is: lane 1 – input (GST-CDK6 beads + p19<sup>INK4d</sup>), lane 2 – supernatant and lane 3 – pellet of pull down. In (A), a – Doubly phosphorylated p19<sup>INK4d</sup>, b – p19<sup>INK4d</sup> as positive control. M – protein molecular weight marker. (B) CDK6-p19<sup>INK4d</sup> complex formation. Overlaid 2D <sup>1</sup>H-<sup>15</sup>N HSQC spectra of <sup>15</sup>N labeled p19<sup>INK4d</sup> before (black) and after addition of unlabeled CDK6 (red). Blue labels indicate residues of p19<sup>INK4d</sup> that interact with CDK6 via their side chains, as revealed by the crystal structure of the complex [17], but which do not influence the back bone chemical shift of p19<sup>INK4d</sup>. Red labels indicate the backbone chemical shift changes upon complex formation both monitored by NMR and reported in the crystal structure. Green labels indicate additional chemical shift changes observed only by NMR and not reported in the crystal structure. These residues are mapped on the structure of p19<sup>INK4d</sup> as shown in the (C). (D) Top image showing autoradiography of lane 1 – untreated p19<sup>INK4d</sup>, lane 2 – p19<sup>INK4d</sup> and lane 3 – CDK6-p19<sup>INK4d</sup> complex treated with S phase cell extract. The upper panel shows the autoradiogram and the corresponding coomassie brilliant blue stained gel below. Middle shows the overlaid 2D <sup>1</sup>H-<sup>15</sup>N HSQC spectra of <sup>15</sup>N labeled p19<sup>INK4d</sup> after the CDK6-p19<sup>INK4d</sup> complex incubated with extract of S phase cells (red) and untreated p19<sup>INK4d</sup> (black). Bottom shows the respective <sup>31</sup>P NMR spectrum and the asterisk indicates the phosphate buffer signal.

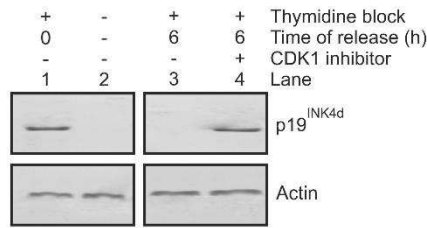


**Figure 5:** Phosphorylation-dependent degradation of endogenous p19<sup>INK4d</sup>. Immunoblot of p19<sup>INK4d</sup> in HeLa cell extracts: lane 1 – S phase cells; lane 2 – asynchronous cells; lane 3 – S phase cells and 6 h after thymidine release; lane 4 – S phase cells at 6 h after thymidine release in the presence of CDK1 inhibitor (upper panel). Actin is shown as loading control (lower panels).

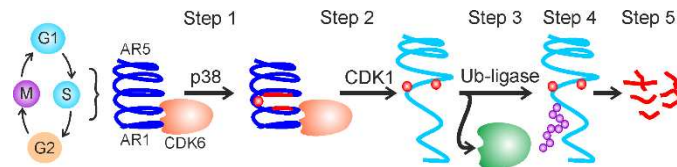


**Figure 6:** Summary of the findings of this study which occur in the S phase of the cell cycle. Step 1: phosphorylation of p19<sup>INK4d</sup> by p38. Step 2 and 3: phosphorylation of p19<sup>INK4d</sup> by CDK1 followed by unfolding of AR1 – AR3 and dissociation of CDK6-p19<sup>INK4d</sup> complex. Step 4: poly ubiquitination of p19<sup>INK4d</sup>. Step 5: degradation of p19<sup>INK4d</sup>.

## Supplementary Information

### Phosphorylation–induced unfolding regulates p19<sup>INK4d</sup> during the human cell cycle

Amit Kumar<sup>1,2,4</sup>, Mohanraj Gopalswamy<sup>1</sup>, Annika Wolf<sup>3</sup>, David J. Brockwell<sup>2</sup>, Mechthild Hatzfeld<sup>3</sup>, Jochen Balbach<sup>\*1,4</sup>

## SI Materials and Methods

**Protein expression and purification.** p19<sup>INK4d</sup> wild type (wt) and mutants were expressed in BL21(DE3) plysS cells and purified as described [43]. Mutations were introduced by using the Stratagene Quikchange kit (Stratagene). The proteins were purified from the soluble protein expression fraction by nickel–NTA column chromatography, followed by gel filtration chromatography (Sephacrose 75), with the exception of S66A and S76A mutants. These mutants were refolded from inclusion bodies. Briefly, cells that had been grown overnight were lysed using a French press after re–suspension in lysis buffer (50 mM sodium phosphate, 50 mM sodium chloride, 1 mM EDTA, and pH 8) containing lysozyme. DNase 1 was added and the mixture was incubated for 30 min at 25 °C. The pellet was collected by centrifugation (20,000 rpm, 4 °C, 20 min.) and washed 3 times with Triton buffer (50 mM sodium phosphate, 150 mM sodium chloride 60 mM EDTA and 6% Triton X–100, pH 8). The pellet was further washed four times with washing buffer (50 mM sodium phosphate, 150 mM sodium chloride, pH 8). The pellet was finally collected by centrifugation and dissolved in solubilizing buffer (50 mM sodium phosphate, 150 mM sodium chloride, 6 M guanidinium hydrochloride, pH 8) and the resulting extract was loaded onto a Ni–NTA column equilibrated with the same buffer. The column was washed and protein was eluted with elution buffer (50 mM sodium phosphate, 150 mM sodium chloride, 6 M guanidinium hydrochloride, pH 4). Refolding of the protein was initiated with rapid dilution in 50 mM sodium phosphate, 150 mM sodium chloride, 100 mM L–arginine, pH 8. Refolded protein was further purified by S–75 gel filtration chromatography. Correct folding was verified by CD and NMR spectroscopy.

**Cell lines and synchronization.** Cervical carcinoma (HeLa), human embryonic kidney 293 (HEK–293) and human osteosarcoma (U2OS) cells, were purchased from ATCC (Manassas, VA, USA). Cell lines were cultured in Dulbecco's modified Eagle medium (DMEM) supplemented with 10 % heat inactivated (56 °C for 30 min) fetal bovine serum (FBS) and 5% (w/v) sodium pyruvate at 37 °C in a humidified chamber with 5 % (v/v) CO<sub>2</sub>. To achieve synchronization of cells, culture dishes were first coated with poly–L–lysine (0.1 mg/ml) for 10 minutes followed by washing twice with phosphate buffer saline (PBS). Cells were then seeded at a density of 0.25 x 10<sup>5</sup> cells / cm<sup>2</sup>. After 7 h, 2.5 mM thymidine was added and incubation was continued for 24 h. Cells were washed with PBS and incubated with fresh medium without thymidine for 12 h. Thymidine was then added at 2.5 mM for 17 h to achieve S–phase synchronization. This medium was replaced with fresh media without thymidine and

the cells were harvested after 3 h (S-phase cells). For M-phase synchronization, cells that had been incubated for 24 h were washed with PBS, followed by addition of fresh medium without thymidine and incubation was continued for 4 h. Nocodazole was then added at 100 nM and incubation was continued for a further 12 h before cells were harvested. To obtain asynchronous cultures, cells were plated at 60 % density and harvested as required. *Drosophila melanogaster* embryos were a kind gift from Gunter Reuter, University of Halle.

**Kinase assay.** Exponentially growing or synchronized cells were washed with PBS and lysed in the presence of protease inhibitor (Sigma-Aldrich, Cat No.-P2714), 2x kinase assay buffer (20 mM MOPS pH 7.5, 15 mM MgCl<sub>2</sub>, 10 mM EGTA, and 2 mM DTT) and phosphatase inhibitors (0.25 mM activated Na<sub>3</sub>VO<sub>4</sub>, 0.5 mM NaF, 15 mM β-glycerophosphate). Cells were lysed by sonication at 10 % amplitude using 3 second pulses and this was performed three times. Lysed cells were centrifuged at 12,000 rpm for 15 minutes at 4 °C. The pellet was discarded and the clear supernatant was used for the kinase reaction. *D. melanogaster* embryo extracts were prepared in the same way without initial PBS washing. The kinase assay was performed by incubating the cell lysate (0.5–1 mg/ml total protein concentration) in the presence of <sup>32</sup>P ATP (5 μCi <sup>32</sup>P-γ-ATP) and cAMP (5 μM) with 30 μg of p19<sup>INK4d</sup> for 3 h at 37 °C. Aliquots of the mixtures were analyzed by SDS-PAGE and labeled polypeptides were detected by autoradiography.

The in vitro kinase assay was performed with isolated p38 or CDK1/cyclin B1 (Sigma Aldrich Pvt. Ltd.). The assay was performed with 5 mM MOPS pH 7.2, 2.5 mM β-glycerophosphate, 10 mM MgCl<sub>2</sub>, 1 mM EGTA, 0.4 mM EDTA, 0.05 mM DTT, 250 ng kinase (CDK1/cyclin B1) or 300 nm (p38), 500 ng protein (p19<sup>INK4d</sup>, p19<sup>INK4d</sup> S76A or p19<sup>INK4d</sup> S66A), and 2 μCi <sup>32</sup>P-γ-ATP. The reaction mixture was incubated at 37 °C for 3 h. Incorporation of radioactivity was detected by autoradiography. The in vitro NMR experiment was also performed in a similar way where 40 μM of <sup>15</sup>N p19<sup>INK4d</sup> and p38α (0.5 μg, Sigma Aldrich Pvt. Ltd.) and/or CDK1/cyclin B (0.5 μg each), 50 μM of ATP, and 5 μM of cAMP were additionally supplemented. These samples were also analyzed by MALDI-TOF mass spectrometry taking the untreated p19<sup>INK4d</sup> as a control.

**NMR spectroscopy experiments.** All NMR spectra were recorded on a Bruker 800 MHz Avance III spectrometer equipped with a CP-TCI cryoprobe at 15 °C and <sup>1</sup>H-<sup>15</sup>N correlations were acquired by 2D FHSQC [44]. The same samples were used to detect the phosphorous

attached to the protein ( $^{31}\text{P}$  NMR) on a Bruker 600 MHz Avance II spectrometer. All spectra were processed using the programs NMRPipe [45] and NMRView [46].

### **Identification of kinases.**

For the identification of the p19<sup>INK4d</sup> kinases, inhibitors were incubated for 10 minutes with lysate prior to addition of p19<sup>INK4d</sup>, ATP and cAMP. The following kinase inhibitors and concentrations were used to identify the respective kinase for Ser66 or Ser76 phosphorylation: CDK1 inhibitor IV RO-3306 [47] at 500 nM, CDK1 inhibitor III CAS 440362-74-3 [48] at 500 nM, CDK2 inhibitor I CVT-313 (48) at 500 nM, protein kinase A (HA 1077, dihydrochloride or fasudil (5-isoquinolinesulfonyl homopiperazine, 2HCl) [49] at 700  $\mu\text{M}$ , p38 inhibitor (SB203580) [50] at 500 nM, CDK4 inhibitor II (1,4-Dimethoxyacridine-9(10H)-thione) [51] at 500 nM. The concentrations indicated above were used in in vitro experiments. Under in vivo conditions, the CDK1 inhibitor (CDK1 inhibitor IV, RO-3306) was used at 35 nM. All the inhibitors were purchase form Merck Millipore Pvt. Ltd, Germany.

**$^1\text{H}/^2\text{H}$  exchange detected by NMR.** The hydrogen-deuterium exchange reaction was started by dissolving lyophilized,  $^{15}\text{N}$  labeled p19<sup>INK4d</sup> in  $^2\text{H}_2\text{O}$  buffer, containing 20 mM sodium phosphate, pD 6.9, 25 mM NaCl and 25 mM KCl. A series of 65  $^1\text{H}$ - $^{15}\text{N}$  HSQC spectra were recorded during an exchange time of 42 h.

**Pull-down assay and CDK6-p19<sup>INK4d</sup> complex.** GST-CDK6 beads were a kind gift from Ernest D. Laue, Cambridge University, UK. p19<sup>INK4d</sup> and GST-CDK6 were dialyzed for 17 h against interaction buffer: 20 mM Na-HEPES, pH 7.5, 150 mM NaCl, 1 mM EDTA, 5 mM DTT, 0.05 % Triton X 100. For the pull-down assay, phosphorylated or control p19<sup>INK4d</sup> (0.5 mg/ml) and 50  $\mu\text{l}$  of a slurry of GST-CDK6 beads were mixed separately (input) and incubated for 45 minutes at 4 °C with gentle rotation. This mixture was centrifuged and the supernatant was used for analysis (supernatant of input). The pellet was washed three times with interaction buffer and finally three times with washing buffer (interaction buffer containing 300 mM NaCl). Aliquots were removed at this step. All samples were analyzed on 12.5 % (w/v) SDS-PAGE.

For the CDK6-p19<sup>INK4d</sup> complex preparation (for NMR spectroscopy analysis), CDK6 was eluted from beads with reduced glutathione. Detached CDK6 and doubly phosphorylated p19<sup>INK4d</sup> or control, untreated p19<sup>INK4d</sup> was dialyzed against interacting buffer. To analyze complex formation, 15  $\mu\text{M}$   $^{15}\text{N}$  labeled p19<sup>INK4d</sup> was added to 17  $\mu\text{M}$  of CDK6. The mixture

was incubated for 17 h and the  $^1\text{H}$ - $^{15}\text{N}$  NMR spectrum was recorded for 24 h.  $\text{p}19^{\text{INK}4\text{d}}$  treated under similar conditions but without CDK6, was used as control for NMR in order to monitor the chemical shift changes upon CDK6 binding. The same complex was treated with cell lysate prepared from S-phase HeLa cells. Additionally, eluted CDK6 was added to the doubly phosphorylated form of  $^{15}\text{N}$  labeled  $\text{p}19^{\text{INK}4\text{d}}$  to analyze the binding by NMR spectroscopy.

**Ubiquitination assays.**  $\text{p}19^{\text{INK}4\text{d}}$  (2  $\mu\text{M}$ ) was incubated with 4 mg/ml of S-phase lysate at 37 °C for 2 h. This mixture was additionally supplemented with the proteasomal inhibitor MG-132 (5  $\mu\text{M}$ ), deconjugating enzyme inhibitor ubiquitin aldehyde (4  $\mu\text{M}$ ), energy regeneration system and ubiquitin solution (600  $\mu\text{M}$ ) purchased from Boston Biochem. Exogenously added phosphorylated or native  $\text{p}19^{\text{INK}4\text{d}}$  was detected by western blotting using mouse monoclonal antibodies (DCS-100) [52] against  $\text{p}19^{\text{INK}4\text{d}}$ .

## SI Figure legends

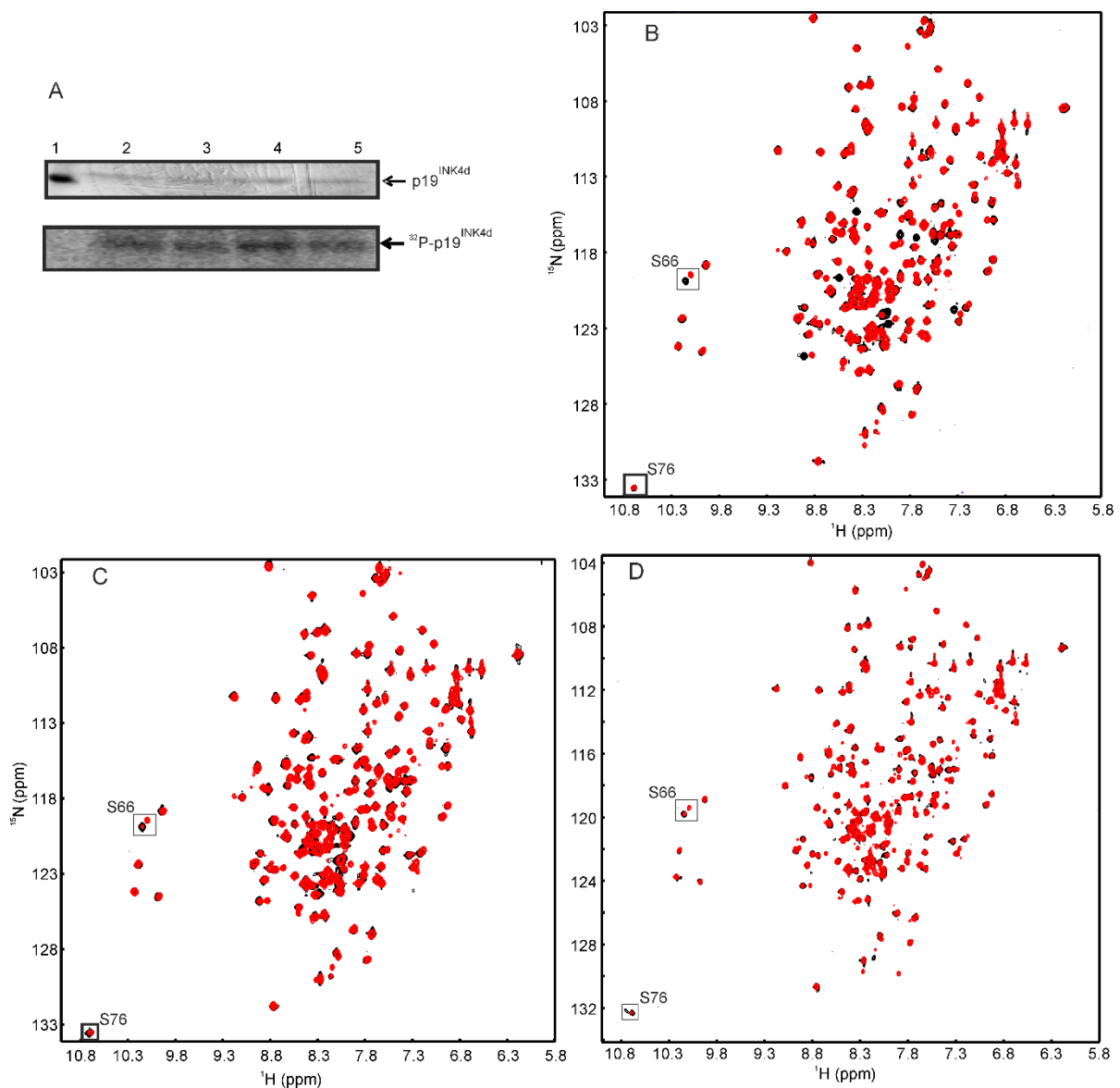


**Fig. S1.** p19<sup>INK4d</sup> phosphorylation by asynchronous cell culture or *D. melanogaster* embryo extracts. (A) The upper panel shows the Coomassie Brilliant Blue stained gel and the lower panel the corresponding autoradiograph. Lane 1 – protein molecular weight marker (19.5 kDa), lane 2 – HeLa cell extract, lane 3 – HEK-293 cell extract, lane 4 – U2OS cell extract, and lane 5 – *D. melanogaster* embryo extract. Fig. (B)–(D) shows superposition of 2D <sup>1</sup>H-<sup>15</sup>N HSQC spectra taken before (black) and after (red) treatment with the extracts. (B) HEK-293 cell extract. (C) U2OS cell extract. (D) *D. melanogaster* embryo extract.

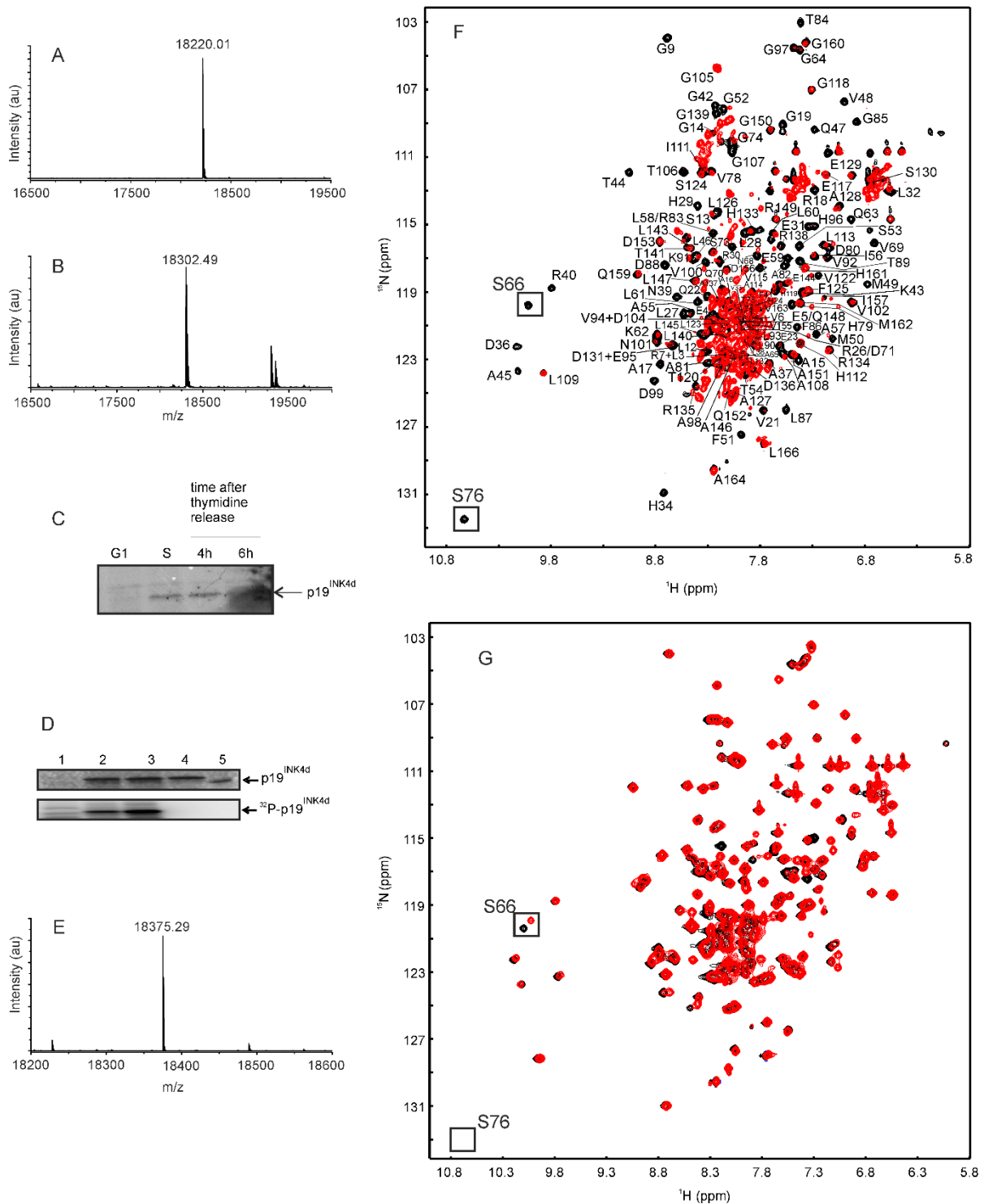


**Fig. S2.** Phosphorylation of p19<sup>INK4d</sup>. (A) MALDI-TOF-MS analysis of untreated p19<sup>INK4d</sup>, (B) Ser66-phosphorylated p19<sup>INK4d</sup> detected by MALDI-TOF-MS; (C) oscillation of p19<sup>INK4d</sup> during cell cycle; (D) p19<sup>INK4d</sup> incubated with S-phase HeLa cell lysate. The upper panel shows the Coomassie Brilliant Blue stained gel and the lower panel indicates the corresponding autoradiograph. Lane 1 – extract alone, lane 2 – p19<sup>INK4d</sup> in the presence of 1 mg/ml extract, lane 3 – p19<sup>INK4d</sup> in the presence of 2 mg/ml extract, lane 4 – untreated p19<sup>INK4d</sup>, and lane 5 – protein molecular weight marker (19.5 kDa). (E) MALDI-TOF-MS analysis of

p19<sup>INK4d</sup> treated with S-phase cell lysate. Indicating double phosphorylation. (F) Ser66 and Ser76 phosphorylated p19<sup>INK4d</sup>. Overlaid <sup>1</sup>H–<sup>15</sup>N 2D HSQC spectra of p19<sup>INK4d</sup> incubated with S-phase HeLa cell lysate (red) and control (black). This figure corresponds to the Fig. 2B in the main text. (G) Overlaid 2D <sup>1</sup>H–<sup>15</sup>N HSQC NMR spectrum of S76A before (black) and after (red) treatment with S-phase cell lysate. This figure corresponds to the Fig. 3F in the main text.

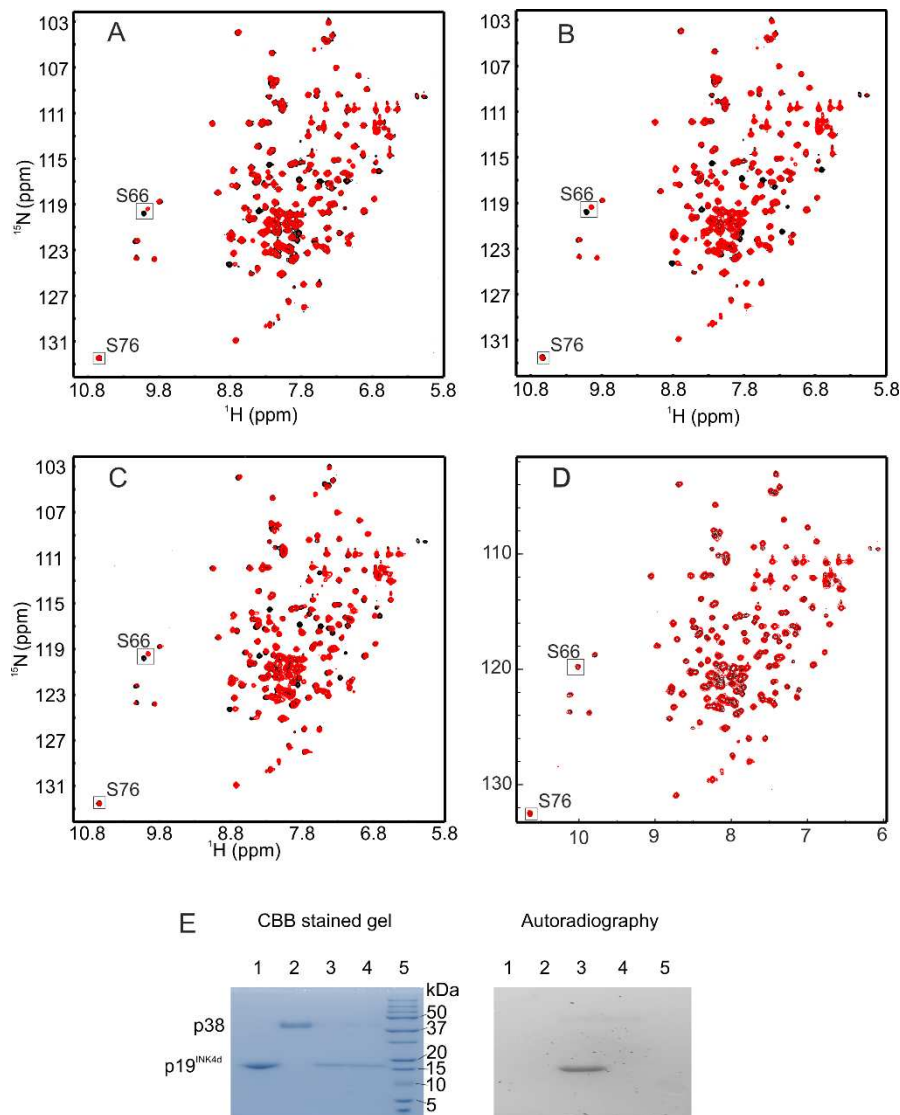


**Fig. S3.** Identification of p38 as a kinase for Ser66 phosphorylation. (A)–(D) Overlaid 2D <sup>1</sup>H–<sup>15</sup>N HSQC spectra of p19<sup>INK4d</sup> treated with HeLa cell lysate (red) and untreated control (black). Inhibitors were incubated with asynchronous cell lysate prior to addition of p19<sup>INK4d</sup>. (A) CDK4 inhibitor II; (B) PKA inhibitor HA 1077; (C) CDK1 inhibitor IV; (D) p38 inhibitor SB203580 (spectrum corresponding to Figure 3E in the main text). (E) in vitro kinase assay with p38 and p19<sup>INK4d</sup>. Left - Coomassie Brilliant Blue stained gel and right – autoradiography image. Lane 1 – p19<sup>INK4d</sup>, lane 2 – p38, lane 3 – p38 + p19<sup>INK4d</sup>, lane 4 – p38 + S66A p19<sup>INK4d</sup>, lane 5 – molecular weight marker.

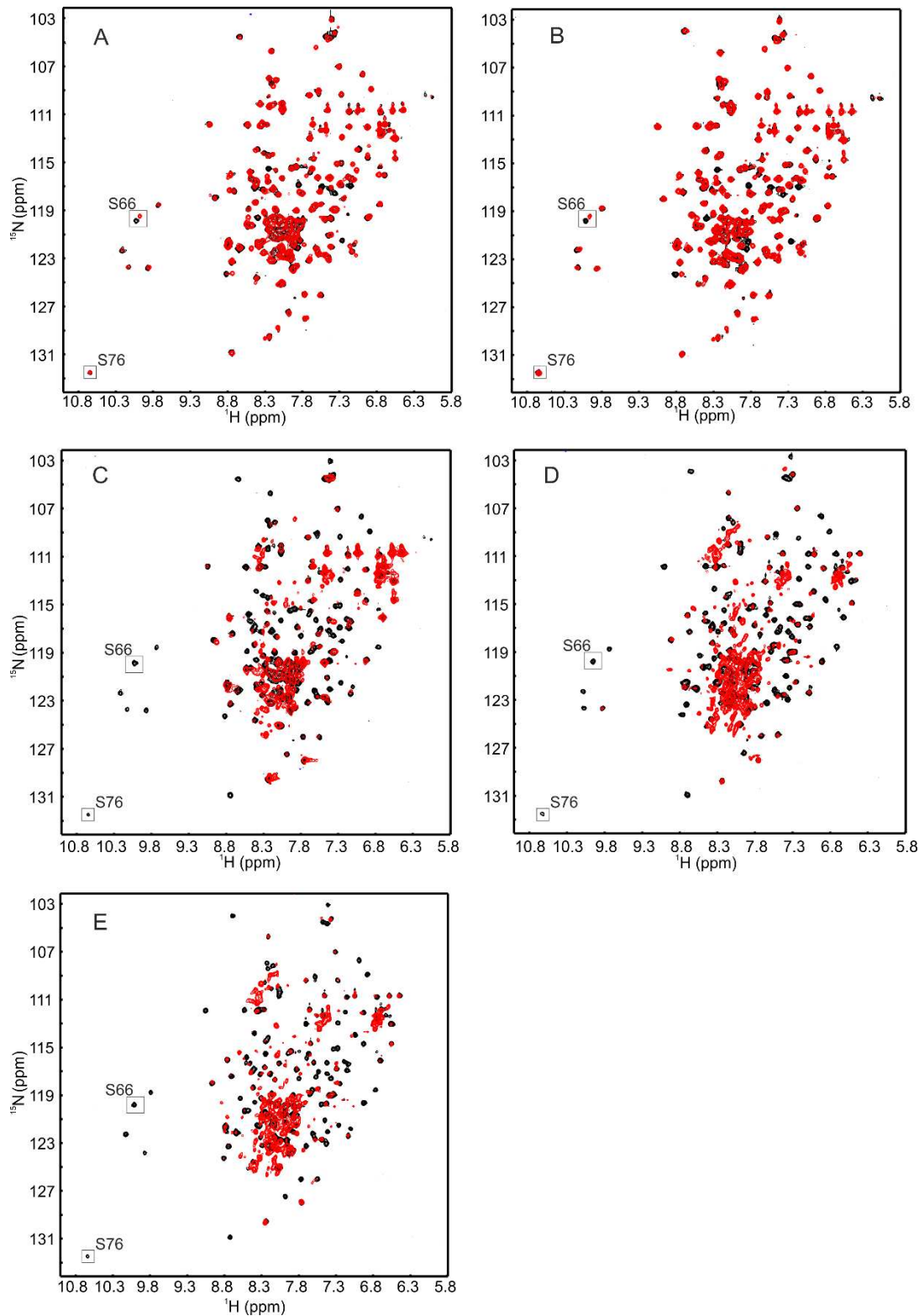


**Fig. S4.** CDK1 is responsible for Ser76 phosphorylation as identified by NMR spectroscopy. Overlaid 2D  $^1\text{H}$ - $^{15}\text{N}$  HSQC spectra before (black) and after (red) treatment with S-phase HeLa cell extract. Inhibitors were incubated with lysate prior to addition of  $^{15}\text{N}$  labeled p19<sup>INK4d</sup>. (A) CKD1 inhibitor IV (corresponds to the Figure 3D in the main text); (B) CDK1 inhibitor III; (C) CDK2 inhibitor I; (D) CDK4 inhibitor II. (E) PKA inhibitor HA 1077.

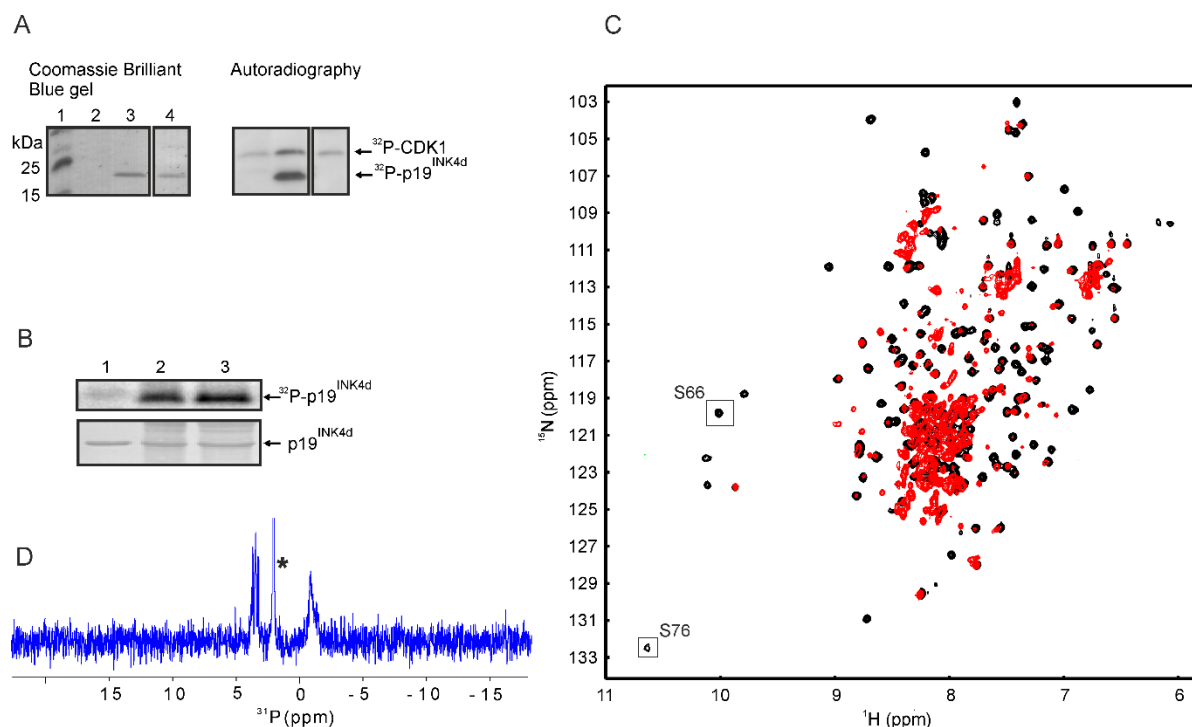


**Fig. S5.** CDK1-mediated phosphorylation of Ser76. (A) In vitro phosphorylation of p19<sup>INK4d</sup> by CDK1/cyclin B. Lane 1 – protein molecular weight marker, lane 2 – CDK1/cyclin B, lane 3 – p19<sup>INK4d</sup> incubated with CDK1/cyclin B, and lane 4 – p19<sup>INK4d</sup> S76A incubated with CDK1/cyclin B. The left panel shows the Coomassie Brilliant Blue stained gel and the right panel the corresponding autoradiographic image. (B) p19<sup>INK4d</sup> treated with lysate, lane 1 – p19<sup>INK4d</sup> alone, lane 2 – S-phase HeLa cell extract, and lane 3 – M-phase cell extract. The upper panel shows an autoradiograph and the lower panel shows the corresponding Coomassie Brilliant Blue stained gel. (C) Overlaid 2D <sup>1</sup>H-<sup>15</sup>N HSQC spectra of p19<sup>INK4d</sup> treated with lysate of M-phase cells (red) and untreated (black). (D) <sup>31</sup>P NMR spectrum of sample (B) showing <sup>31</sup>P resonances of the two protein-bound phosphorylation sites at 4 ppm (Ser76) and -1 ppm (Ser66). The asterisk indicates the signal of the phosphate buffer.

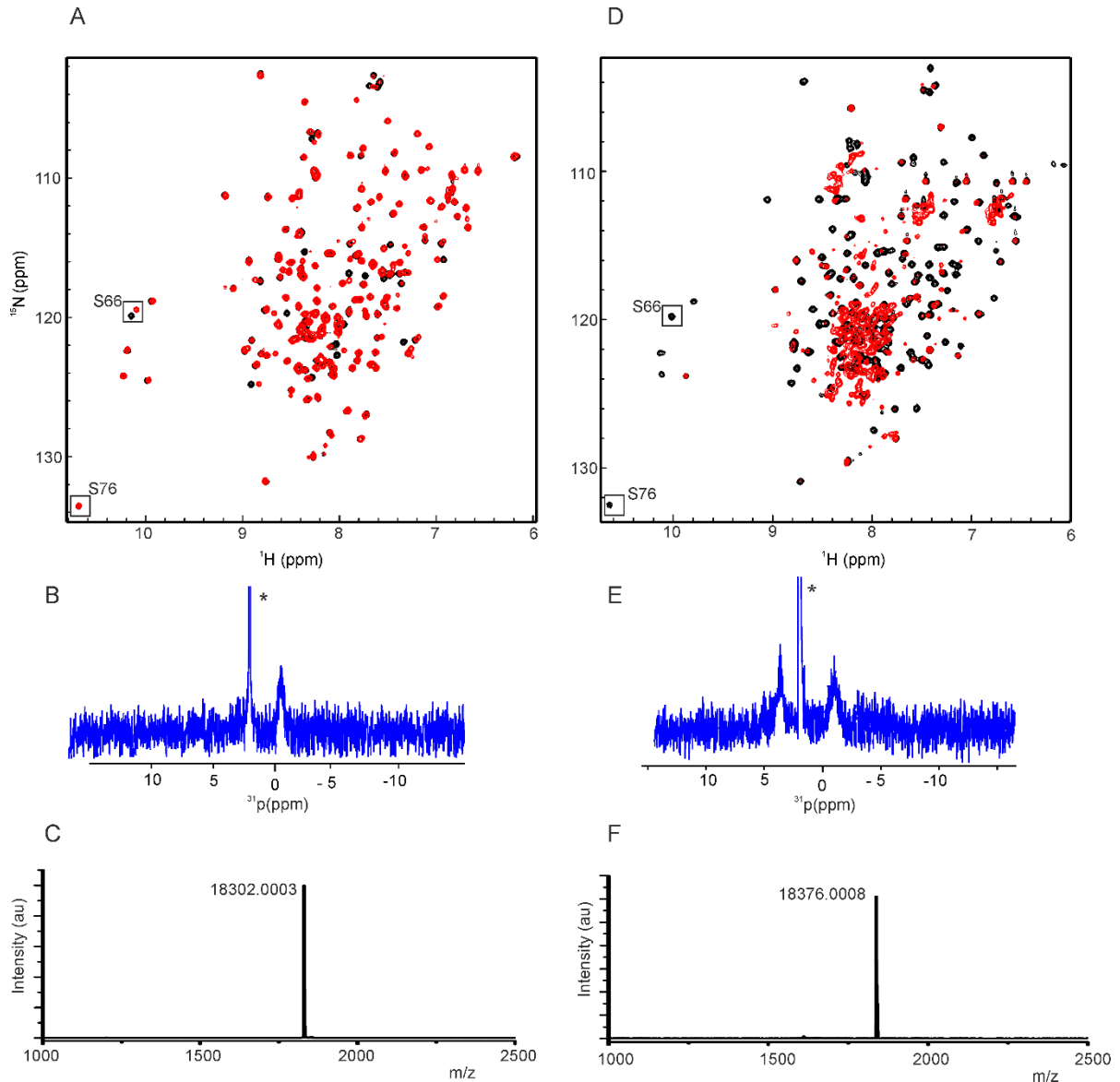


**Fig. S6:** In vitro phosphorylation of p19 using an isolated kinase. (A) p19<sup>INK4d</sup> incubated with p38 $\alpha$ . Overlaid 2D <sup>1</sup>H–<sup>15</sup>N HSQC spectra of p19<sup>INK4d</sup> treated with p38 (red) and untreated (black). (B) <sup>31</sup>P NMR spectrum of sample (A) showing <sup>31</sup>P resonances of one protein phosphorylation site at –1 ppm (Ser66). (C) MALDI-TOF-MS analysis of the sample used in (A). (D) p19<sup>INK4d</sup> incubated with p38 $\alpha$  and CDK1-cyclin B. Overlaid 2D <sup>1</sup>H–<sup>15</sup>N HSQC spectra of p19<sup>INK4d</sup> treated with p38 $\alpha$  and CDK1-cyclin B (red); and untreated (black). (E) <sup>31</sup>P NMR spectrum of sample (D) showing <sup>31</sup>P resonances of the two protein phosphorylation sites at 4 ppm (Ser76) and –1 ppm (Ser66). (F) MALDI-TOF-MS analysis of the samples used in (D). In (B) and (E) asterisk indicates the signal of the phosphate buffer.

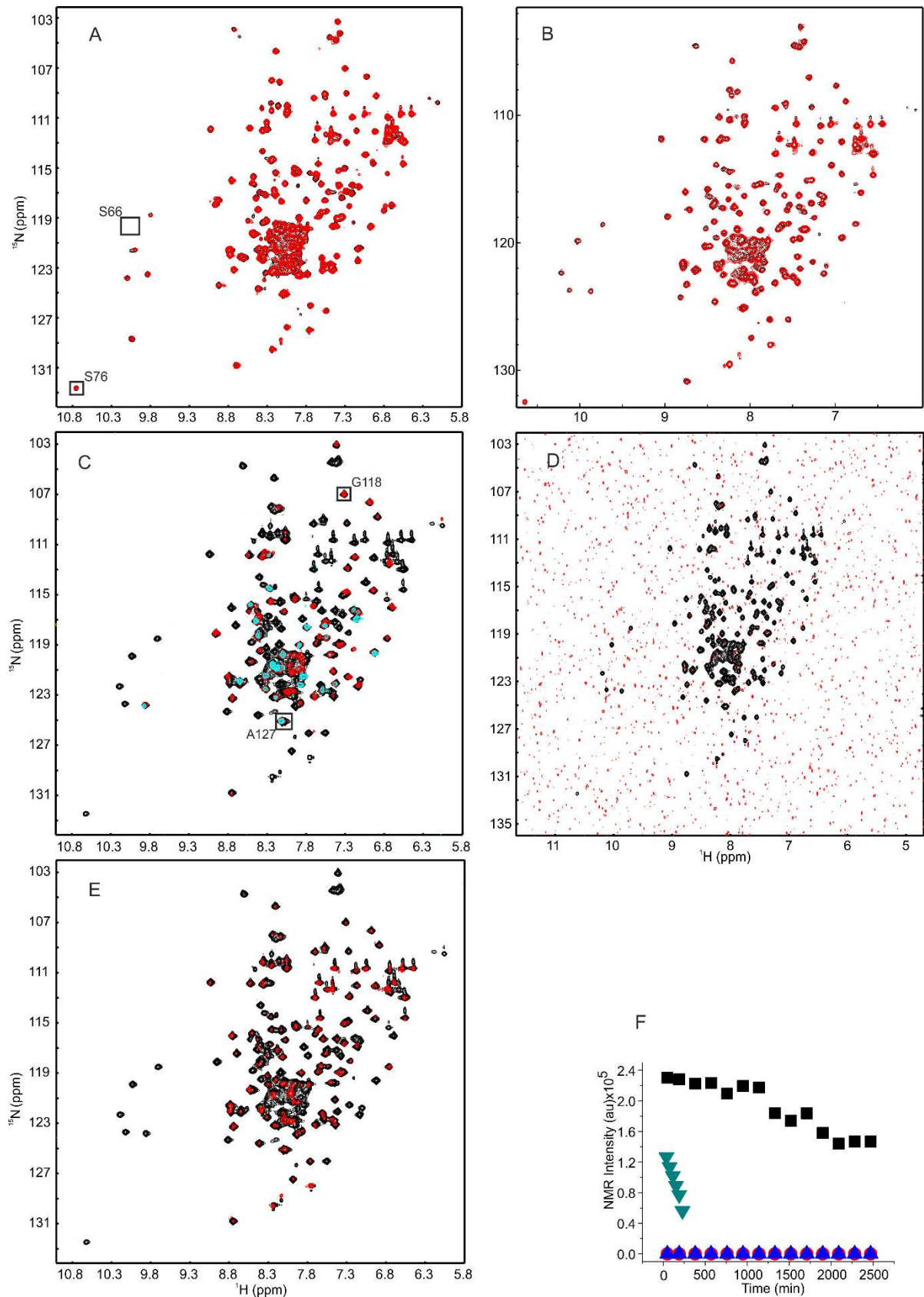


**Fig. S7.** Sequential phosphorylation of p19<sup>INK4d</sup>. Overlaid 2D <sup>1</sup>H-<sup>15</sup>N HSQC spectra of p19<sup>INK4d</sup> treated with S-phase HeLa cell lysate (red) and untreated (black). (A) S66A variant of p19<sup>INK4d</sup> (the spectrum corresponds to Figure 3G in the main text). (B) Wild type p19<sup>INK4d</sup> in the presence of p38 inhibitor (the spectrum corresponds to Figure 3H in the main text). (C)

– (D) NMR detected  $^1\text{H}/^2\text{H}$  exchange of amide protons of  $\text{p}19^{\text{INK}4\text{d}}$  and the Ser66 phosphoprotein. (C) Exchange experiment with unmodified  $^{15}\text{N}$   $\text{p}19^{\text{INK}4\text{d}}$ . The black spectrum was recorded at pH 6.9 (reference), the red spectrum was recorded 10 min after dissolving lyophilized protein in  $^2\text{H}_2\text{O}$ , pD 6.9, and the cyan spectrum was recorded after 42 h of exchange. (D) Exchange experiment with the Ser66 phosphoprotein, where all cross-peaks are missing after 10 min of  $^2\text{H}_2\text{O}$  exposure (red spectrum, lower contour level) because of the global destabilization of  $\text{p}19^{\text{INK}4\text{d}}$ . The black spectrum was recorded in  $\text{H}_2\text{O}$  at pH 6.9. (E) Indicates reappearance of the cross-peaks of Ser66 phosphorylated  $\text{p}19^{\text{INK}4\text{d}}$  of initially fully deuterated protein after addition of 30 % of buffer in  $\text{H}_2\text{O}$  (red). (F) Shows the time-course of  $^1\text{H}/^2\text{H}$  exchange of representative cross-peaks: ■ – A127 and ▼ – G118 represent untreated  $\text{p}19^{\text{INK}4\text{d}}$ , while ▲ – A127 and ● – G118 represent  $\text{p}19^{\text{INK}4\text{d}}$  with phosphorylated Ser66.

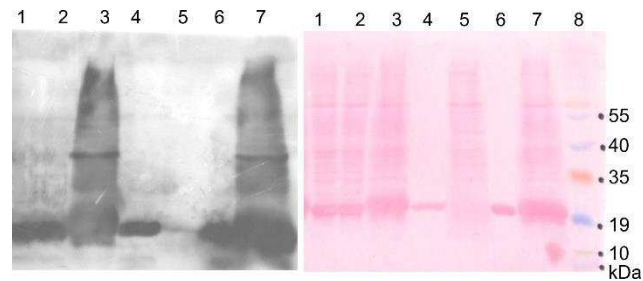


**Fig. S8.** Ubiquitination of  $\text{p}19^{\text{INK}4\text{d}}$ . Ubiquitination assay of  $\text{p}19^{\text{INK}4\text{d}}$ . The left panel depicts the Western blot analysis of  $\text{p}19^{\text{INK}4\text{d}}$  detected by a monoclonal antibody against  $\text{p}19^{\text{INK}4\text{d}}$  (DCS 100): lane 1 –  $\text{p}19^{\text{INK}4\text{d}}$  Ser66 phosphorylated, lane 2 –  $\text{p}19^{\text{INK}4\text{d}}$  S76A (phosphorylated), lane 3 –  $\text{p}19^{\text{INK}4\text{d}}$  doubly phosphorylated, lane 4 –  $\text{p}19^{\text{INK}4\text{d}}$  S76A (control), lane 5 – cell extract, lane 6 –  $\text{p}19^{\text{INK}4\text{d}}$  wt (control), lane 7 –  $\text{p}19^{\text{INK}4\text{d}}$  doubly phosphorylated (duplicate reaction). The right panel shows Ponceau S staining of the membrane depicted on the left side and lane 8 shows the molecular weight marker.

## SI References

1. Sherr CJ 1996 Cancer cell cycles *Science* **274** 1672.
2. Zwicker J, Liu N, Engeland K, Lucibello FC, & Muller R 1996 Cell cycle regulation of E2F site occupation in vivo *Science* **271** 1595.
3. Wu CL, Zukerberg LR, Ngwu C, Harlow E, & Lees JA 1995 In vivo association of E2F and DP family proteins *Mol Cell Biol* **15** 2536.
4. Kim HY & Cho Y 1997 Structural similarity between the pocket region of retinoblastoma tumour suppressor and the cyclin-box *Nat Struct Biol* **4** 390.
5. Korenjak M & Brehm A 2005 E2F-Rb complexes regulating transcription of genes important for differentiation and development *Curr Opin Genet Dev* **15** 520.
6. Das SK, et al. 2005 Fucoxanthin induces cell cycle arrest at G0/G1 phase in human colon carcinoma cells through up-regulation of p21WAF1/Cip1 *Biochim Biophys Acta* **1726** 328.
7. Morgan DO 1995 Principles of CDK regulation *Nature* **374** 131.
8. Weinberg RA 1995 The retinoblastoma protein and cell cycle control *Cell* **81** 323.
9. Harper JW & Elledge SJ 1996 Cdk inhibitors in development and cancer *Curr Opin Genet Dev* **6** 56.
10. Pines J 1996 Cell cycle: reaching for a role for the Cks proteins *Curr Biol* **6** 1399.
11. Thullberg M, Bartek J, & Lukas J 2000 Ubiquitin/proteasome-mediated degradation of p19INK4d determines its periodic expression during the cell cycle *Oncogene* **19** 2870.
12. Ito Y & Selenko P 2010 Cellular structural biology *Curr Opin Struct Biol* **20** 640.
13. Selenko P, et al. 2008 In situ observation of protein phosphorylation by high-resolution NMR spectroscopy *Nat Struct Mol Biol* **15** 321.
14. Theillet FX, et al. 2016 Structural disorder of monomeric alpha-synuclein persists in mammalian cells *Nature* **530** 45.
15. Theillet FX, et al. 2013 Site-specific NMR mapping and time-resolved monitoring of serine and threonine phosphorylation in reconstituted kinase reactions and mammalian cell extracts *Nat Protoc* **8** 1416.
16. Kumar A, et al. 2014 N-terminal phosphorylation of parathyroid hormone (PTH) abolishes its receptor activity *ACS Chem. Biol.* **9** 2465.
17. Brotherton DH, et al. 1998 Crystal structure of the complex of the cyclin D-dependent kinase Cdk6 bound to the cell-cycle inhibitor p19INK4d *Nature* **395** 244.
18. Baumgartner R, et al. 1998 Structure of human cyclin-dependent kinase inhibitor p19(INK4d): comparison to known ankyrin-repeat-containing structures and implications for the dysfunction of tumor suppressor p16(INK4a) *Structure* **6** 1279.
19. Whitfield ML, et al. 2002 Identification of genes periodically expressed in the human cell cycle and their expression in tumors *Mol Biol Cell* **13** 1977.
20. Forget A, et al. 2008 Differential post-transcriptional regulation of two Ink4 proteins, p18 Ink4c and p19 Ink4d *Cell Cycle* **7** 3737.
21. Cuadrado A & Nebreda AR 2010 Mechanisms and functions of p38 MAPK signalling *The Biochemical journal* **429** 403.
22. Cuenda A & Rousseau S 2007 p38 MAP-kinases pathway regulation, function and role in human diseases *Biochimica et biophysica acta* **1773** 1358.
23. Zarubin T & Han J 2005 Activation and signaling of the p38 MAP kinase pathway *Cell research* **15** 11.
24. Marazita MC, et al. CDK2 and PKA mediated-sequential phosphorylation is critical for p19INK4d function in the DNA damage response *PLoS One* **7** e35638.

25. Vassilev LT, et al. 2006 Selective small-molecule inhibitor reveals critical mitotic functions of human CDK1 *Proc Natl Acad Sci USA* **103** 10660.
26. Brachwitz K, et al. 2003 Evaluation of the first cytostatically active 1-aza-9-oxafluorenes as novel selective CDK1 inhibitors with P-glycoprotein modulating properties *J Med Chem* **46** 876.
27. Hochegger H, et al. 2007 An essential role for Cdk1 in S phase control is revealed via chemical genetics in vertebrate cells *J Cell Biol* **178** 257.
28. Satyanarayana A & Kaldis P 2009 Mammalian cell-cycle regulation: several Cdks, numerous cyclins and diverse compensatory mechanisms *Oncogene* **28** 2925.
29. Hochegger H, Takeda S, & Hunt T 2008 Cyclin-dependent kinases and cell-cycle transitions: does one fit all? *Nat Rev Mol Cell Biol* **9** 910.
30. Holt LJ, et al. 2009 Global analysis of Cdk1 substrate phosphorylation sites provides insights into evolution *Science* **325** 1682.
31. Löw C, et al. 2007 Folding mechanism of an ankyrin repeat protein: scaffold and active site formation of human CDK inhibitor p19(INK4d) *J Mol Biol* **373** 219.
32. Kong SK & Chock PB 1992 Protein ubiquitination is regulated by phosphorylation. An in vitro study *J Biol Chem* **267** 14189.
33. Nguyen LK, Kolch W, & Kholodenko BN 2013 When ubiquitination meets phosphorylation: a systems biology perspective of EGFR/MAPK signalling *Cell Commun Signal* **11** 52.
34. Thullberg M, et al. 2000 Distinct versus redundant properties among members of the INK4 family of cyclin-dependent kinase inhibitors *FEBS Lett* **470** 161.
35. Löw C, Homeyer N, Weininger U, Sticht H, & Balbach J 2009 Conformational switch upon phosphorylation: human CDK inhibitor p19INK4d between the native and partially folded state *ACS Chem Biol* **4** 53.
36. Cervantes CF, Handley LD, Sue SC, Dyson HJ, & Komives EA 2013 Long-range effects and functional consequences of stabilizing mutations in the ankyrin repeat domain of I $\kappa$ B $\alpha$  *J Mol Biol* **425** 902.
37. Barrick D 2009 Biological regulation via ankyrin repeat folding *ACS Chem Biol* **4** 19.
38. Löw C, et al. 2008 Structural insights into an equilibrium folding intermediate of an archaeal ankyrin repeat protein *Proc Natl Acad Sci USA* **105** 3779.
39. Diaz-Moreno I, et al. 2009 Phosphorylation-mediated unfolding of a KH domain regulates KSRP localization via 14-3-3 binding *Nat Struct Mol Biol* **16** 238.
40. Venkataramani R, Swaminathan K, & Marmorstein R 1998 Crystal structure of the CDK4/6 inhibitory protein p18INK4c provides insights into ankyrin-like repeat structure/function and tumor-derived p16INK4 mutations *Nat Struct Biol* **5** 74.
41. Flory E, Hoffmeyer A, Smola U, Rapp UR, & Bruder JT 1996 Raf-1 kinase targets GA-binding protein in transcriptional regulation of the human immunodeficiency virus type 1 promoter *J Virol* **70** 2260.
42. Gupta S & Sen S 2002 Myotrophin- $\kappa$ B DNA interaction in the initiation process of cardiac hypertrophy *Biochim Biophys Acta* **1589** 247.
43. Löw C, et al. 2007 Folding mechanism of an ankyrin repeat protein: scaffold and active site formation of human CDK inhibitor p19(INK4d) *J. Mol. Biol.* **373** 219.
44. Mori S, Abeygunawardana C, Johnson MO, & van Zijl PC 1995 Improved sensitivity of HSQC spectra of exchanging protons at short interscan delays using a new fast HSQC (FHSQC) detection scheme that avoids water saturation *J. Magn. Reson. B* **108** 94.
45. Delaglio F, et al. 1995 NMRPipe: a multidimensional spectral processing system based on UNIX pipes *J. Biomol. NMR* **6** 277.

46. Johnson BA 2004 Using NMRView to visualize and analyze the NMR spectra of macromolecules *Methods Mol. Biol.* **278** 313.
47. Vassilev LT, et al. 2006 Selective small-molecule inhibitor reveals critical mitotic functions of human CDK1 *Proc. Natl. Acad. Sci.* **103** 10660.
48. Brachwitz K, et al. 2003 Evaluation of the first cytostatically active 1-aza-9-oxafluorenes as novel selective CDK1 inhibitors with P-glycoprotein modulating properties *J. Med. Chem.* **46** 876.
49. Watanabe K, et al. 2007 A ROCK inhibitor permits survival of dissociated human embryonic stem cells *Nat. Biotechnol.* **25** 681.
50. Rasmussen MH, et al. 2016 miR-625-3p regulates oxaliplatin resistance by targeting MAP2K6-p38 signalling in human colorectal adenocarcinoma cells *Nat. Commun.* **7**.
51. Kubo A, et al. 1999 The p16 status of tumor cell lines identifies small molecule inhibitors specific for cyclin-dependent kinase 4 *Clin. Cancer Res.* **5** 4279.
52. Thullberg M, et al. 2000 Distinct versus redundant properties among members of the INK4 family of cyclin-dependent kinase inhibitors *FEBS Lett.* **470** 161.